CHEMISTRY
A EUROPEAN JOURNAL

DOI: 10.1002/chem.200902050

Persistent Mixed-Valence $[(TTF)_2]^{+\bullet}$ Dyad of a Chiral Bis(binaphthol)–tetrathiafulvalene (TTF) Derivative

Ali Saad,[a] Frédéric Barrière,[a] Eric Levillain,[b] Nicolas Vanthuyne,[c] Olivier Jeannin,[a] and Marc Fourmigué*[a]

Abstract: Mixed-valence dyadic $[(TTF)_2]^{+\bullet}$ (TTF = tetrathiafulvalene) species—the elementary building blocks of organic conductors—are usually too weakly associated to be observed in solution, unless covalently bound in dimers or physically constrained into a cage structure. We demonstrate here that a novel chiral tetrathiafulvalene functionalised with two 1,1′-binaphthol units (**1**) is able to associate in solution into persistent mixed-valence $[(TTF)_2]^{+\bullet}$ dyadic moieties through a stereospecific recognition pattern. This redox active molecule exhibits different electrochemical and spectroscopic responses, as enantiopure *RR*, *SS* or *meso* isomers, a rare example of a chiral system in which different diastereoisomers do not exhibit the same electrochemical features, with a selective formation of the mixed-valence species in the enantiopure (*RR*)-**1** or (*SS*)-**1** isomers only, whereas the *meso* form does not show this association ability. A rationale for the selective self-association of the *RR* and *SS* enantiomers upon oxidation is provided, based on the different molecular geometries and accessibility of the TTF core toward the formation of the mixed-valence species.

Keywords: chirality · electrochemistry · radical ions · self-assembly · tetrathiafulvalene

Introduction

Molecular conductors derived from the redox-active tetrathiafulvalene molecule (TTF)[1] are most often based on the infinite stacking of an elementary building block, the mixed-valence $[(TTF)_2]^{+\bullet}$ species. Within such a dyad with radical cation character, the bonding and anti-bonding combinations of the two TTF HOMOs are, respectively, doubly and singly occupied, a situation that gives a 0.5 bond-order character to the intermolecular interaction within the cationic dyad. As a consequence, these mixed-valence species are only weakly associated, and thus most often not directly observable in solution. A notable exception involves the case of arenes (naphthalene, fluoranthene, and so on) at high concentration and low temperature.[2] The only rare examples in which such a mixed-valence $[(TTF)_2]^{+\bullet}$ species has been observed in solution are restricted to situations in which the two TTF moieties are forced to interact, either when covalently linked into TTF dimers[3] or cyclophanes,[4] or embedded within a cage, as an organic cucurbit[8]uril receptor[5] or a self-assembled coordination cage.[6] Besides these two situations, a stable self-association of TTF moieties within a $[(TTF)_2]^{+\bullet}$ mixed-valence species has not been observed yet, but can be anticipated if specific non-covalent intermolecular interactions can simultaneously stabilise the dyadic association and hinder its precipitation. We describe here a novel TTF derivative in which a stable, persistent, mixed-valence $[(TTF)_2]^{+\bullet}$ state has been identified upon chemical and electrochemical oxidation. Furthermore, the specific recognition pattern observed within these non-covalent $[(TTF)_2]^{+\bullet}$ dyads finds here its origin in the chirality of this TTF molecule, based on the atropoisomerism of binaphthol units. Indeed, chiral tetrathiafulvalenes are currently being developed for the introduction of chirality in molecular conductors.[7–9] We postulated that the introduction, on a tetrathiafulvalene core, of chiral 1,1′-binaphthol moieties,

[a] A. Saad, Dr. F. Barrière, Dr. O. Jeannin, Dr. M. Fourmigué
Sciences Chimiques de Rennes, Université de Rennes 1
CNRS UMR 6226, Campus de Beaulieu, 35042 Rennes (France)
Fax: (+33) 223-23-67-32
E-mail: marc.fourmigue@univ-rennes1.fr

[b] Dr. E. Levillain
Laboratoire CIMA, Université d'Angers
CNRS UMR 6200, 2 Bd. Lavoisier, 49042 Angers (France)

[c] Dr. N. Vanthuyne
UMR 6263 - ISM2 - Université Paul Cézanne
Avenue Escadrille Normandie Niémen, 13397 Marseille cedex 20 (France)

Supporting information for this article is available on the WWW under http://dx.doi.org/10.1002/chem.200902050.

available with very high enantiomeric purity,[10] would favour chiral solid-state organisations through a combination of π–π interactions and overlap interactions of open-shell molecules. We describe here the synthesis and electrochemical properties of the symmetrically substituted tetrathiafulvalene (TTF) derivative **1**, as diastereomeric mixture (*RR*, *SS*, *meso*) as well as pure *RR*, *SS* and *meso* isomers. The peculiar geometrical features of **1** allowed for the favoured formation of an unprecedented homochiral mixed-valence aggregate $[(\mathbf{1})_2]^{+\bullet}$ upon oxidation.

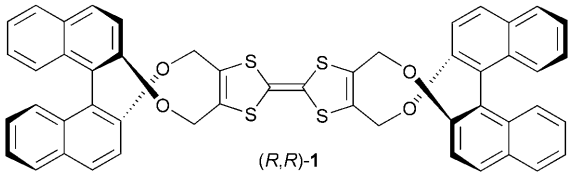

Results and Discussion

Only a few TTF derivatives that incorporate a binaphthyl moiety have been described to date. They are all based on a single binaphthol platform that bears a TTF moiety coupled to each naphthalene ring, through either conjugated[11] or non-conjugated linkers,[12,13] thereby affording in all cases highly flexible molecules with two TTF moieties per binaphthol unit. Such optically active derivatives were described as chiral molecular switches through circular dichroism modulation upon oxidation,[12] and were used for the formation of intramolecular dyads.[11,13] The synthesis of **1** (Scheme 1) involves a completely different route, as it is based on the NEt_3 coupling reaction of the dithiolium cation **6**. The latter was obtained in three steps from the 1,3-dithiole-2-thione **3**. The key step is the preparation of **3**, which was successfully obtained in high yield from the alkylation of 1,1′-binaphthol with 3,4-bis(bromomethyl)-1,3-dithiole-2-thione[14] in high dilution conditions. Such conditions were required to avoid the extensive formation of polymeric insoluble material, in competition with the targeted formation of the rigid ten-membered ring in **3**. All reactions were performed with either enantiopure (*R*)-, (*S*)- or racemic (*R*,*S*)-1,1′-binaphthol, thereby affording the dithiolium cation **6** as enantiopure (*R*)-**6** or (*S*)-**6** and racemic (*R*,*S*)-**6**. The symmetrical cross-coupling reaction of (*R*)-**6** or (*S*)-**6** with NEt_3 in CH_3CN hence afforded the enantiopure (*RR*)-**1** or (*SS*)-**1**, respectively (Figure 1). On the other hand, the diastereomeric mixture (*RR*,*SS*,*meso*)-**1** was obtained from the coupling of the racemic (*R*,*S*)-**6**.

Concentration of a solution of the diastereoisomeric mixture (*RR*,*SS*,*meso*)-**1** in CH_2Cl_2 allowed for the selective precipitation of the *meso* form, a favourable situation, as this *meso* isomer cannot be prepared in a simple way by the symmetrical cross-coupling strategy of dithiolium cations presented above in Scheme 1. Chiral HPLC analyses showed the high purity of the precipitated *meso* form and confirmed that the mother liquors were indeed strongly enriched in the racemic mixture (see the Supporting Information). Attempts to crystallise the pure *RR* or *SS* enantiomers or the diastereomeric mixture were unsuccessful and X-ray powder diffraction showed that the samples were amorphous. On the other hand, the *meso* derivative afforded single crystals amenable to X-ray diffraction analysis. Derivative *meso*-**1** crystallises in the triclinic system, space group $\bar{P}1$, with four crystallographically independent molecules, each of them located on a inversion centre together with

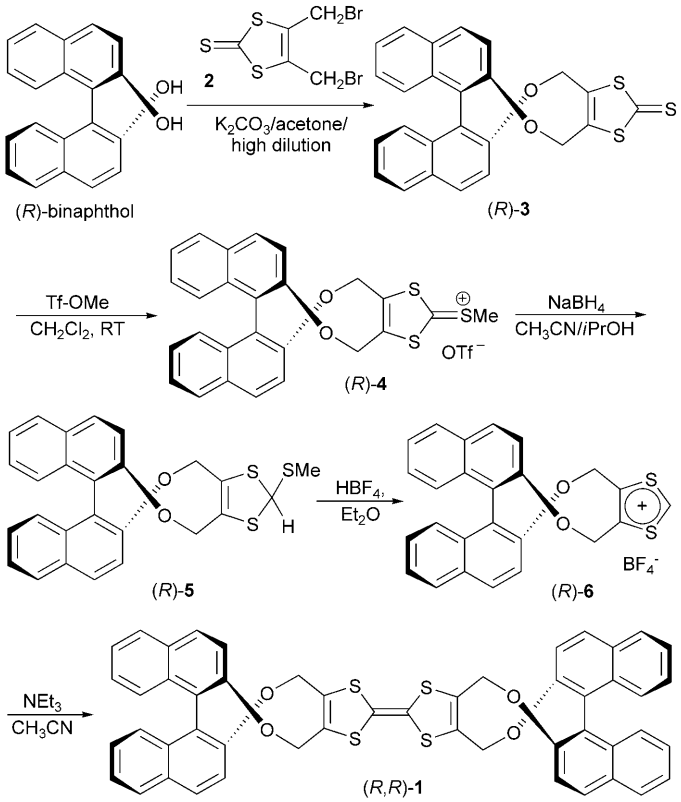

Scheme 1. Synthetic path to (*R*,*R*)-**1** (Tf = triflate).

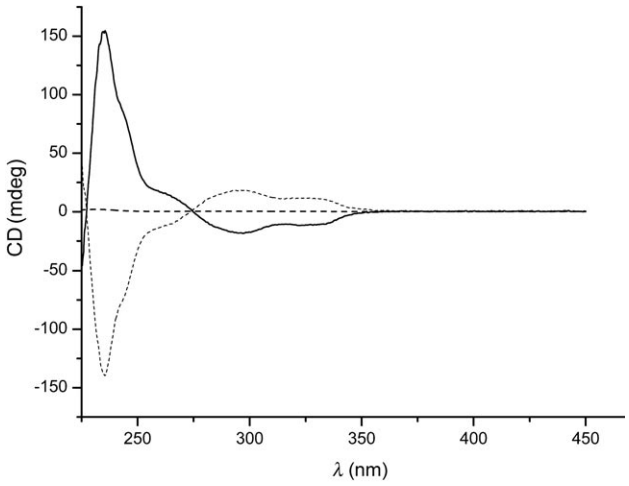

Figure 1. Circular dichroism spectra for (*RR*)-**1** (——) and (*SS*)-**1** (-----) (5×10^{-5} M in CH_2Cl_2).

two acetone molecules in general position, hence a 1:1 [*meso*-**1**]·acetone stoichiometry for this solvate. As shown in Figure 2, the TTF moiety is essentially planar, with small

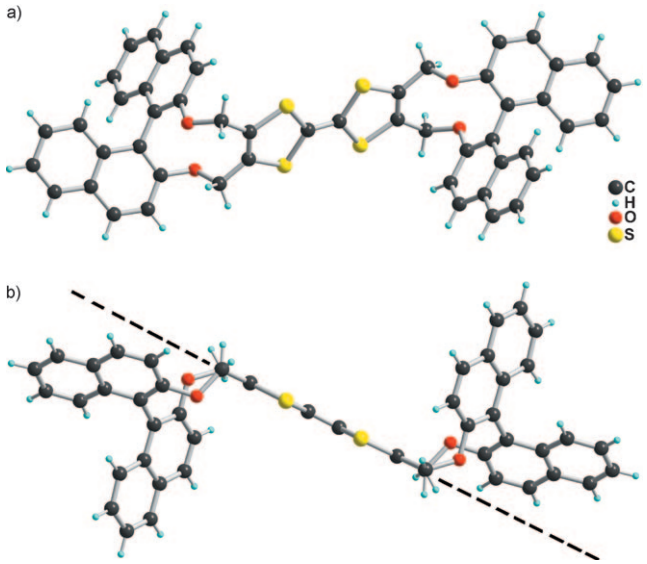

Figure 2. a) Molecular structure of one of the four crystallographically independent molecules in [*meso*-**1**]·acetone. b) A side view showing that the binaphthol moiety is located fully above or below the TTF molecular plane (dotted line).

distortions of the dithiole ring characterised by a folding along the S···S hinge, frequently observed in neutral TTF derivatives (1.5(2), 15.5(3), 0.0(2) and 0.1(2)°, in crystallographically independent molecules A, B, C and D, respectively). The binaphthol moiety adopts a *cisoid* conformation imposed by the constrained ten-membered ring, with a dihedral angle between the two naphthyl rings that amounts to 63.8(1), 71.6(1), 69.9(1) and 64.4(1)° in molecules A, B, C and D, respectively. Note also that the binaphthol moieties are located in full above or below the TTF molecular plane (dotted line in Figure 2b).

Cyclic voltammetry (CV) experiments (Figure 3a) performed on the *meso* form show the classical two-wave behaviour characteristic of monomeric TTF derivatives, and related to the sequential oxidation of *meso*-**1** to the mono and dicationic species. This is also confirmed by the deconvoluted cyclic voltamogramm (Figure 3a, right) with two identical processes. On the other hand, one observes a surprising broadening of the first oxidation wave in the diastereomeric mixture (Figure 3b), a behaviour even more clearly identified in the voltamogramm (and deconvoluted voltamogramm) of the enantiopure (*RR*)-**1** (Figure 3c) or (*SS*)-**1** (see the Supporting Information) in which the first oxidation wave is now clearly split into two waves.

Such splitting of the first oxidation wave is usually characteristic of the favoured formation of an intermediate mixed-valence TTF dyad $(TTF)_2^{+\bullet}$, a species only rarely observed in a few TTF dimers and cyclophanes in which the two TTF are either covalently linked,[3,4] or when constrained within cagelike rigid structures.[5,6] A glycoluril-based TTF covalent dyad that associates into clip dimers under oxidative control provides another recent rare example.[15] The splitting of the first oxidation wave observed here in the enantiopure (*RR*)-**1** or (*SS*)-**1** molecules that bear a single TTF moiety implies that, upon electron transfer, a stabilising non-covalent interaction between two molecules allows for a persistent dyadic mixed-valence species, and that this supramolecular association is efficient only in the enantiopure (*RR*)-**1** or (*SS*)-**1** molecules but not in the *meso* form. The intermediate situation observed in the diasteroisomeric mixture represents then an average of both extreme behaviours. This splitting of the first oxidation process of TTF derivatives is coherent with the well-known "square scheme".[16,17] To estimate the binding constants for the formation of the mixed-valence $[(TTF)_2]^{+\bullet}$ (K_{MV}) and $[(TTF)_2]^{2+}$ dimer (K_{Dim}), the square scheme requires a scan rate and/or concentration dependence during experimental CV. However (and as expected for TTF derivatives), the experimental CV of (*RR*)-**1** or (*SS*)-**1** is scan-rate and concentration independent under our conditions, thereby suggesting that the kinetic constants of the binding constants are very fast. An alternative is to use of the value of the potential splitting (ΔE), but ΔE depends on the K_{MV} and K_{Dim} ratio, according to Equation (1) in which R is the gas constant, T is the temperature, n is the number of electrons and F is the Faraday constant. Consequently, the binding constants for the formation of the dimer and the mixed-valence species could not be estimated from electrochemical experiments.

$$\Delta E = RT/nF \ln(K_{MV}/K_{Dim}) \quad (1)$$

To confirm this striking difference of behaviour between the isomers, UV/Vis near-infrared (NIR) investigations were also carried out after the chemical oxidation of either (*RR*)-**1**, (*SS*)-**1** or *meso*-**1** and the diastereoisomeric mixture (*RR*,*SS*,*meso*)-**1**, by addition of $NOSbF_6$ aliquots. As shown in Figure 4, in addition to the UV/Vis absorption bands attributable to the radical cation species, an extra absorption band is observed above 2000 nm after addition of 0.5 equiv $NOSbF_6$, but only in the enantiopure (*RR*)-**1** or (*SS*)-**1** molecules, whereas it is completely absent in the *meso* isomer and notably weakened in the diastereoisomeric mixture. This 2000 nm band is characteristic of an inter-valence absorption band[18] and confirms therefore that an association of two TTF moieties into non-covalent dyads does occur upon oxidation of the TTF core to give a persistent mixed-valence $(TTF)_2^{+\bullet}$ species, but only in the enantiopure *RR* or *SS* molecules, whereas it is not allowed in the *meso* compound. In other words, we are here in the presence of a chiral system in which different diastereoisomers do not exhibit the same electrochemical features, with a favoured formation of the mixed-valence species in the enantiopure (*RR*)-**1** or (*SS*)-**1** isomers, whereas the *meso* form does not show this association ability.

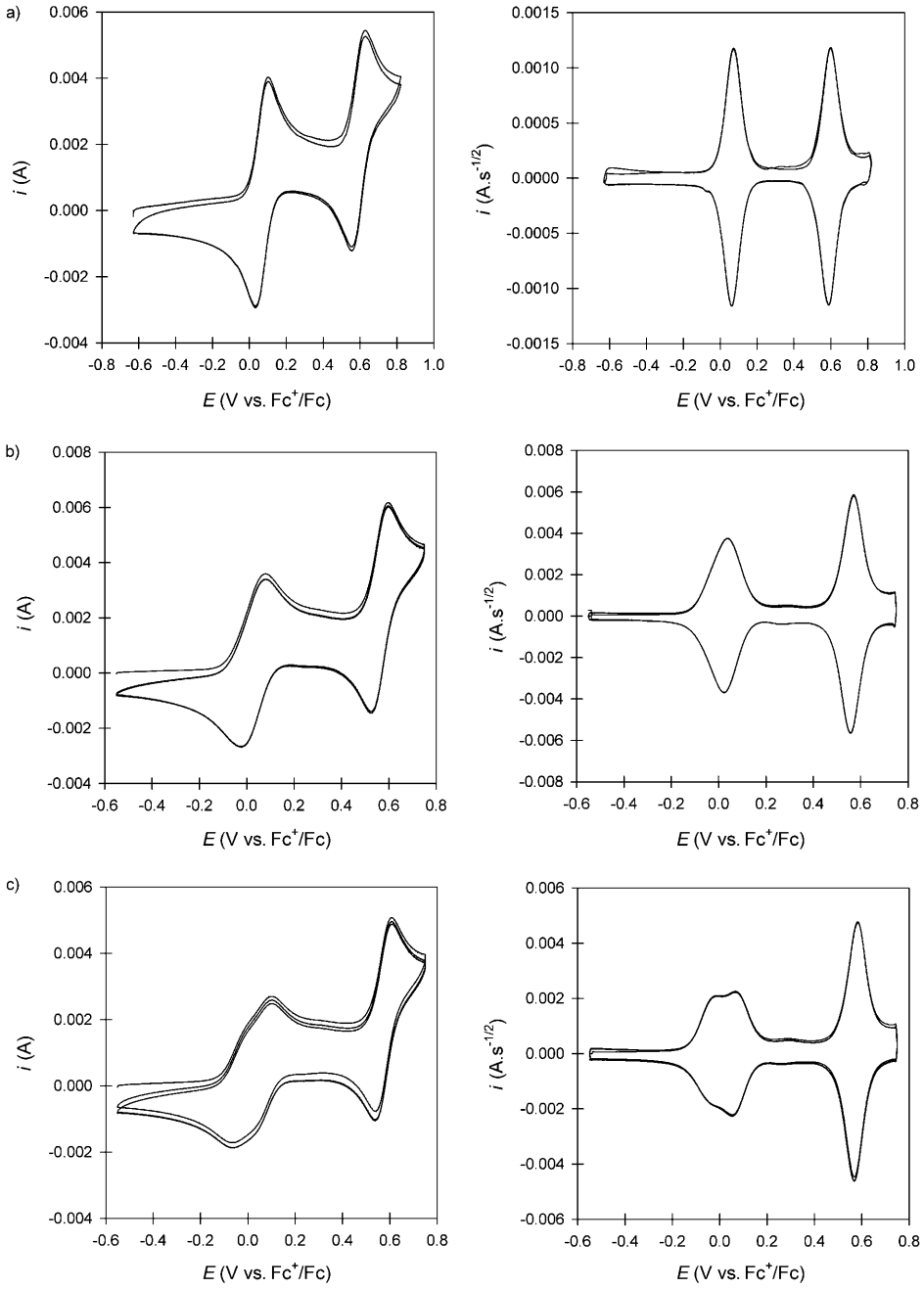

Figure 3. Experimental (left) and deconvoluted (right) cyclic voltammetry for a) *meso*-**1**, b) the diastereomeric (*RR*,*SS*,*meso*)-**1** mixture and c) the enantiopure (*RR*)-**1** enantiomer (0.5 mM solutions in CH_2Cl_2 with 0.1 M nBu$_4$NPF$_6$).

At this stage, geometrical models of the molecule in its different stereoisomers and conformers are clearly needed to offer a rationale for this striking behaviour. Based on the geometry of *meso*-**1** determined experimentally (see above), a model geometry of the TTF derivatives (*RR*)-**1** or (*SS*)-**1** can be anticipated in both boat and chair conformations. Indeed, these two conformations are possibly obtained from the cross-coupling reaction of dithiolium cations **6** and are known to exchange rapidly in solution in the presence of acid traces[19] or upon oxidation by rotation around the weakened central C=C bond. Geometry optimisations with density functional theory (DFT; B3LYP/6-31G*) were performed on both the boat and chair conformations of (*RR*)-**1** as well as on *meso*-**1**, in their neutral and cation radical state (Figure 5), thus showing near identical energy for the two conformers in each oxidation state.

Furthermore, as shown in Figure 6, the molecule isomers in their boat conformation clearly exhibit two distinct geometries related to the relative orientations of two naphthyl arms that protrude at right angles out of the TTF plane. In the *RR* and *SS* enantiomers, the two arms are parallel, thus leaving an open and deep chasm in between. By contrast, in the *meso* form, the two naphthyl arms mirror each other and the canyon in between is now shut at one end. In summary, the two naphthyl arms appear here as swivel doors, thereby defining a rather wide and parallel channel in the *RR* and *SS* enantiomers, whereas, in the *meso* isomer, it is half-closed at one end by a narrow strait.

As we are looking for a possible stabilising intermolecular interaction to rationalise the spectroscopic and electrochemical observations, several association patterns of the two molecules upon oxidation can be considered, depending on their boat or chair conformation. Among possible association patterns, the self-association of the *RR* isomer into an interlocked homochiral structure $[\{(RR)\text{-}\mathbf{1}\}_2]^{+\bullet}$ depicted in Figure 7 is likely to explain the selective association of the *RR* or *SS* isomers. Indeed, the distance between the two parallel naphthyl planes is large enough to accommodate a second TTF moiety, at variance with the *meso* isomer, which seems to preclude this aggregate formation. Note that this model also allows a (*RR*)-**1**/(*SS*)-**1** enantiomer association and offers a rationale for the observed spectroscopic data upon chemical oxidation.

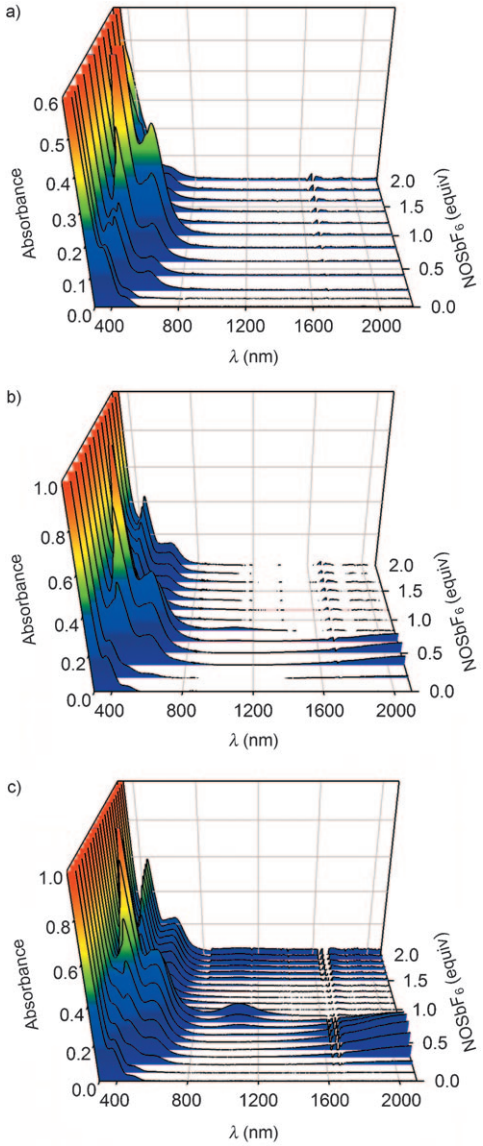

Figure 4. UV/Vis NIR spectra (0.5 mM in CH_2Cl_2) of a) the *meso*-**1** isomer , b) the diastereoisomeric (*RR*,*SS*,*meso*)-**1** mixture and c) the enantiopure (*RR*)-**1** upon $NOSbF_6$ oxidation.

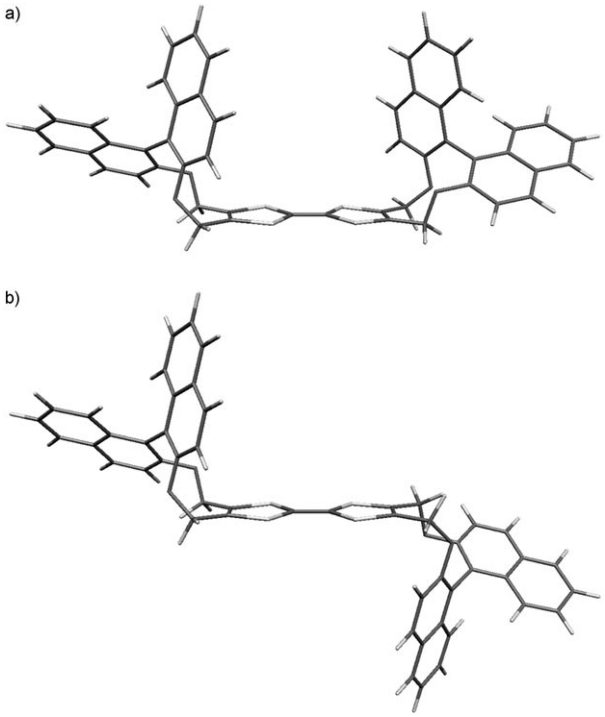

Figure 5. Optimised geometries in the cation radical state for a) the boat and b) the chair conformation of (*RR*)-**1**. In the neutral state, similar geometries are obtained with usual distortions from planarity of the dithiole rings.

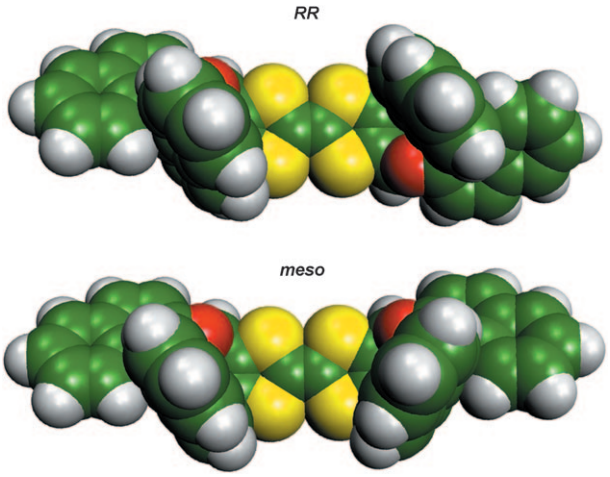

Figure 6. Optimised geometry in the cation radical state and boat conformation for the two diastereoisomers (*RR*)-**1** and *meso*-**1**, which shows the parallel orientation of the protruding naphthyl rings in (*RR*)-**1** that opens a deep valley in between, whereas the mirroring naphthyl rings in *meso*-**1** hinder any strong face-to-face approach of the TTF redox cores on this side.

Indeed, within the diastereomeric mixture only half on the molecules, the (*RR*)-**1** and (*SS*)-**1** can form persistent mixed-valence aggregates with themselves and between them, whereas the *meso* isomer cannot.

DFT geometry optimisations for such an interlocked structure [{(*RR*)-**1**}$_2$] were performed both in the neutral and in the mixed-valence cation state. The optimised geometry for [{(*RR*)-**1**}$_2$]$^{+\bullet}$ shown in Figure 7 demonstrates that the interlocking is not only possible, but strongly favoured as the energy difference between that of this mixed-valence dyad [{(*RR*)-**1**}$_2$]$^{+\bullet}$ and the sum of individual neutral (*RR*)-**1** and cationic [(*RR*)-**1**]$^{+\bullet}$ amounts to 16 kcal mol^{-1}.[20] The same geometry optimisation for the neutral interlocked dyad converged toward a similar geometry, but with a larger plane-to-plane distance between the TTF moieties (i.e., 4.2 vs. 3.9 Å) and a much lower energy gain (2 kcal mol^{-1}) when compared with the energy of two isolated neutral (*RR*)-**1** molecules. It should be stressed also that this pattern of association of two TTF moieties with their long axis almost perpendicular to each other also allows for a strong overlap between TTF HOMOs, as illustrated in Figure 7 (bottom).

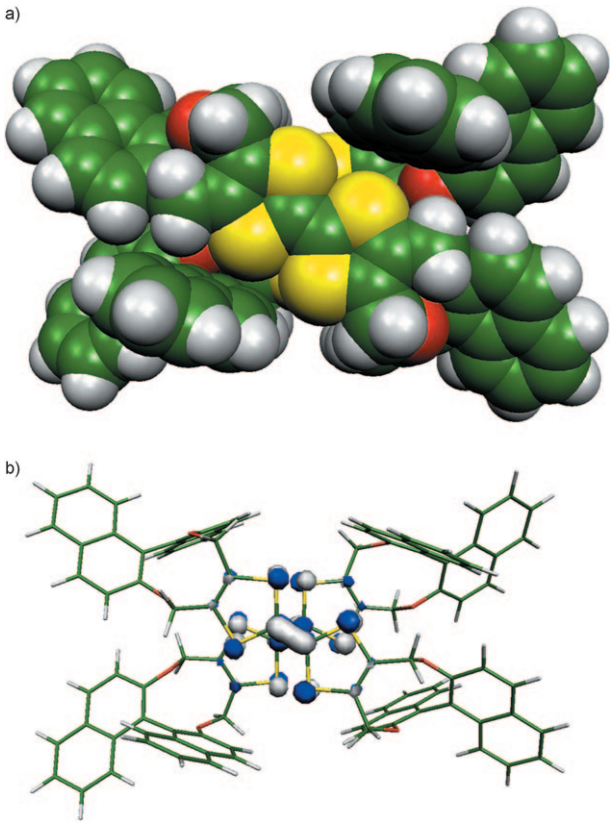

Figure 7. a) Optimised geometry, in its mixed-valence state, of the bimolecular homochiral aggregate $[\{(RR)\text{-}\mathbf{1}\}_2]^{+\bullet}$. b) HOMO of the mixed-valence dyadic cationic species $[\{(RR)\text{-}\mathbf{1}\}_2]^{+\bullet}$.

This overlap pattern is quite rare and has been reported only in criss-cross bis-TTF cyclophanes in which the relative arrangement of the two TTF cores was once again rigidly constrained by covalent bonds.[21]

Calculations were also performed on the dyads formed by two (*RR*)-**1** molecules, now in back-to-back geometries, with the TTF moieties facing each other through a criss-cross or an eclipsed overlap conformation. In these situations in which all stabilising interactions associated to the interlocking are absent, the relative calculated energies again show a stabilisation of the aggregate in the mixed-valence state albeit in a significantly lower extent than in the interlocked geometry (9 vs. 16 kcal mol^{-1}).

Conclusion

The formation of a persistent mixed-valence species $[(TTF)_2]^{+\bullet}$, characterised by its NIR absorption above 2000 nm, has been reported up to now only in TTF dimers when covalently linked or embedded within a cage structure. We have shown here that, among the three components ((*RR*)-**1**, (*SS*)-**1** and *meso*-**1**) of a diastereomeric mixture of original redox-active, chiral or binaphthol TTF derivatives, each of them in isoenergetic and interconverting boat or chair conformations, a high degree of molecular recognition could be attained in solution upon electron transfer toward the formation of a mixed-valence dyad that involves exclusively the (*RR*)-**1** and (*SS*)-**1** enantiomers. The chirality brought by the atropoisomerism of binaphthol units combined with the rigidity of these substituents has allowed here for an unprecedented self-association of TTF derivatives upon oxidation through a process able to discriminate between diastereoisomers.

Experimental Section

Preparation of (*R,S*)-3: A mixture of racemic (*R,S*)-1,1′-binaphthol (3.22 g, 0.0112 mol), 4,5-bis(bromomethyl)-2-thioxo-1,3-dithiole (**2**; 3.6 g, 0.0112 mmol) and K_2CO_3 (15.8 g) in acetone (2.8 L) was heated at reflux under argon for 24 h with mechanical stirring. After evaporation of acetone in vacuo, the residue was solubilised in water (3 L)/CH_2Cl_2 (3 L). The decanted organic phase was washed with aqueous 10% NaOH (2 × 750 mL), aqueous 2 N HCl (1.5 L) and H_2O (2.5 L), dried over $MgSO_4$, filtered and evaporated in vacuo. The crude product was dissolved in CH_2Cl_2, and petroleum ether was added. The resulting solution was left at 4 °C overnight, and the precipitated solids were filtered, washed with petroleum ether and air-dried to give (*R,S*)-**3** as a yellow powder. Yield: 4 g (80%). M.p. 272–273 °C; ^{1}H NMR (300 MHz, CD_2Cl_2): δ = 7.93 (d, J = 9 Hz, 2H), 7.83 (d, J = 8.4 Hz, 2H), 7.36 (d, J = 9 Hz, 2H), 7.34–7.28 (m, 2H), 7.18–7.13 (m, 2H), 7.04–7.00 (m, 2H), 4.96 ppm (s, 4H); ^{13}C NMR (75 MHz, CD_2Cl_2): δ = 210.16, 154.07, 140.69, 133.93, 130.72, 130.48, 128.63, 127.16, 126.14, 125.08, 122.59, 117.67, 64.25 ppm; MS (MALDI-TOF): m/z: 444.67 [M^+]; elemental analysis calcd (%) for $C_{25}H_{16}O_2S_3$: C 67.54, H 3.63; found: C 67.12, H 3.44.

Preparation of (*R*)-3: A mixture of enantiopure (*R*)-1,1′-binaphthol (4.919 g, 0.0171 mol), **2** (5.5 g, 0.0171 mmol) and K_2CO_3 (24.1 g) in acetone (4.2 L) was stirred and heated at reflux under argon for 24 h. The reaction was treated as described for (*R,S*)-**3**. Recrystallisation from toluene/pentane gave (*R*)-**3** as orange crystals. Yield: 6.2 g (84%). M.p. 245 °C; ^{1}H NMR (300 MHz, CD_2Cl_2): δ = 8.05 (d, J = 9 Hz, 2H), 7.96 (d, J = 8.1 Hz, 2H), 7.48 (d, J = 9 Hz, 2H), 7.46–7.41 (m, 2H), 7.31–7.25 (m, 2H), 7.18–7.15 (m, 2H), 5.02 ppm (s, 4H); ^{13}C NMR (75 MHz, CD_2Cl_2): δ = 210.13, 154.11, 140.70, 133.95, 130.73, 130.51, 128.67, 127.21 126.18, 125.11, 122.59, 117.68, 64.22 ppm; MS (MALDI-TOF): m/z: 444.75 [M^+]; $[\alpha]_D^{20}$ = +112 (c = 0.05 in CH_2Cl_2); elemental analysis calcd (%) for $C_{25}H_{16}O_2S_3$: C 67.54, H 3.63; found: C 67.53, H 3.87.

Preparation of (*S*)-3: A mixture of enantiopure (*S*)-1,1′-binaphthol (4.47 g, 0.0156 mol), **2** (5 g, 0.0156 mol) and K_2CO_3 (21.9 g) in acetone (3.8 L) was stirred and heated at reflux under argon for 24 h. The reaction was treated as described for (*R,S*)-**3**. Recrystallisation from toluene/pentane gave (*S*)-**3** as orange crystals. Yield: 5.5 g (80%). M.p. 243 °C; ^{1}H NMR (300 MHz, CD_2Cl_2): δ = 8.05 (d, J = 9 Hz, 2H), 7.96 (d, J = 8.1 Hz, 2H), 7.47 (d, J = 9 Hz, 2H), 7.46–7.41 (m, 2H),7.31–7.25 (m, 2H), 7.19–7.16 (m, 2H), 5.02 ppm (s, 4H); ^{13}C NMR (75 MHz, CD_2Cl_2): δ = 210.14, 154.11, 140.70, 133.95, 130.73, 130.52, 128.69, 127.22, 126.18, 125.12, 122.58, 117.67, 64.21 ppm; $[\alpha]_D^{20}$ = −114 (c = 0.05 in CH_2Cl_2); MS (MALDI-TOF): m/z : 444.5 [M^+]; elemental analysis calcd (%) for $C_{25}H_{16}O_2S_3$: C 67.54, H 3.63; found: C 66.51, H 3.61.

Preparation of (*R,S*)-4: Methyl trifluoromethanesulfonate (1 mL, 9.5 mmol) was added at room temperature to a solution of (*R,S*)-**3** (2 g, 4.49 mmol) in anhydrous CH_2Cl_2 (150 mL) under nitrogen. The resulting solution was stirred for 6 h. Anhydrous Et_2O (250 mL) was then added, and the solution was left at 4 °C overnight. The yellow precipitate was filtered to give (*R,S*)-**4**. Yield: 4 g (88%). M.p. 190 °C; ^{1}H NMR (300 MHz, CD_3CN): δ = 8.06 (d, J = 8.7 Hz, 2H), 7.9 (d, J = 8.1 Hz, 2H), 7.64 (d, J = 9 Hz, 2H), 7.43–7.37 (m, 2H), 7.25–7.20 (m, 2H), 7.02 (d, J = 8.7 Hz, 2H), 5.55–5.43 (AA′, J = 13.8 Hz, 4H; -CH_2-), 3.00 ppm (s, 3H);

^{13}C NMR (75 MHz, CD_3CN): δ = 204.51, 153.14, 149.26, 132.95, 130.07, 129.98, 128.03, 126.63, 125.10, 124.50, 121.25, 117.04, 116,91, 62.99, 22.91 ppm; elemental analysis calcd (%) for $C_{27}H_{19}F_3O_5S_4$: C 53.28, H 3.15; found: C 51.62, H 3.04. The product is unstable and must be stored at low temperature.

Preparation of (*R*)-4: Methyl trifluoromethanesulfonate (0.6 mL, 5.7 mmol) was added at room temperature to a solution of (*R*)-**3** (2 g, 4.49 mmol) in anhydrous CH_2Cl_2 (15 mL) under nitrogen. The resulting solution was stirred for 4 h. Anhydrous Et_2O (50 mL) was then added, and the solution was left at 4 °C overnight. After removal of the ethereal liquid, the resulting oil was dried under vacuum to yield (*R*)-**4** as orange crystals. Yield: 2.6 g (95 %). M.p. 135 °C; ^{1}H NMR (300 MHz, $CDCl_3$): δ = 7.84 (d, *J* = 9 Hz, 2H), 7.75 (d, *J* = 8.4 Hz, 2H), 7.54 (d, *J* = 9 Hz, 2H), 7.29 (t, *J* = 7.6 Hz, 2H), 6.99–7.09 (m, 4H), 5.38–5.60 (AA′, *J* = 13.8 Hz, 4H; $-CH_2-$), 2.83 ppm (s, 3H); ^{1}H NMR (75 MHz, CD_3CN): δ = 8.01 (d, *J* = 9 Hz, 2H), 7.91 (d, *J* = 8.1 Hz, 2H), 7.64 (d, *J* = 9 Hz, 2H), 7.39–7.34 (m, 2H), 7.20–7.14 (m, 2H), 7.00 (d, *J* = 8.4 Hz, 2H), 5.56–5.45 (AA′, *J* = 13.8 Hz, 4H, -CH_2-), 2.97 ppm (s, 3H); ^{13}C NMR (300 MHz, $CDCl_3$): δ = 202.74, 153.29, 150.08, 133.40, 130.53, 130.32, 128.27, 126.96, 125.86, 124.98, 121.76, 118.37, 116.92, 63.47, 23.29 ppm; $[\alpha]_D^{20} = -12$ (*c* = 0.05 in CH_2Cl_2); elemental analysis calcd (%) for $C_{27}H_{19}F_3O_5S_4$: C 53.28, H 3.15; found: C 51.87, H 2.99. The product is unstable and must be stored at low temperature.

Preparation of (*S*)-4: Methyl trifluoromethanesulfonate (1 mL, 9.5 mmol) was added at room temperature to a solution of (*S*)-**3** (2.5 g, 5.6 mmol) in anhydrous CH_2Cl_2 (20 mL) under nitrogen. The resulting solution was stirred for 4 h, anhydrous Et_2O (100 mL) was then added, and the solution was left at 4 °C overnight. After removal of the ethereal liquid, the resulting oil was dried under vacuum to yield (*S*)-**4** as orange crystals. Yield: 3.2 g (94 %). M.p. 138 °C; ^{1}H NMR (300 MHz, CD_3CN): δ = 8.02 (d, *J* = 9 Hz, 2H), 7.91 (d, *J* = 8.1 Hz, 2H), 7.63 (d, *J* = 9 Hz, 2H), 7.40–7.34 (m, 2H), 7.21–7.15 (m, 2H), 7.01 (d, *J* = 8.4 Hz, 2H), 5.56–5.44 (AA′, *J* = 13.8 Hz, 4H; -CH_2-), 2.96 ppm (s, 3H); ^{13}C NMR (75 MHz, CD_3CN): δ = 204.51, 153.16,149.29, 132.97, 130.05, 129.98, 128.01, 126.61, 125.09, 124.50, 121.28, 117.03, 116.91, 63.06, 22.91 ppm; $[\alpha]_D^{20} = +10$ (*c* = 0.05 in CH_2Cl_2); elemental analysis calcd (%) for $C_{27}H_{19}F_3O_5S_4$: C 53.28, H 3.15; found: C 52.15, H 3.32.

Preparation of (*R,S*)-5: $NaBH_4$ (0.13 g, 3.28 mmol) was cautiously added to a solution of the dithiolium salt (*R,S*)-**4** (2 g, 3.28 mmol) in anhydrous CH_3CN (30 mL) and *i*PrOH (2 mL) under nitrogen at 0 °C. The mixture was allowed to reach room temperature and stirred for 4 h. Purification by column chromatography (silica gel, petroleum ether/EtOAc 10:2) afforded (*R,S*)-**5** as beige crystals after drying. Yield: 1.3 g (86 %). M.p. 135 °C; ^{1}H NMR (300 MHz, $CDCl_3$): δ = 8.00 (d, *J* = 9 Hz, 1H), 7.96 (d, *J* = 9 Hz, 1H), 7.88 (d, *J* = 9 Hz, 2H), 7.53 (d, *J* = 9 Hz, 1H), 7.33–7.40 (m, 3H), 7.11–7.26 (m, 4H), 5.92 (s, 1H), 4.95–4.76 (AA′BB′, 4H; -CH_2-), 1.80 ppm (s, 3H); ^{13}C NMR (75 MHz, $CDCl_3$): 154.43, 154.03, 133.71, 130.29, 130.09, 129.73, 129.67, 128.17, 128.04, 127.21, 126.60, 126.58, 126.48, 126.18, 126.15, 124.37, 122.51, 122.28, 117.76, 117.53, 65.27, 64.63, 59.07, 11.04 ppm; MS (MALDI-TOF): *m*/*z*: 460.69 [M^+]; elemental analysis calcd (%) for $C_{26}H_{20}O_2S_3$: C 67.79, H 4.38; found: C 67.31, H 4.89.

Preparation of (*R*)-5: As described above for (*R,S*)-**5**. Yield: 1.35 g (90 %). M.p. 128 °C; ^{1}H NMR (300 MHz, $CDCl_3$): δ = 8.00 (d, *J* = 9 Hz, 1H), 7.96 (d, *J* = 8.7 Hz, 1H), 7.88 (d, *J* = 9 Hz, 2H), 7.53 (d, *J* = 9 Hz, 1H), 7.33–7.40 (m, 3H), 7.11–7.26 (m, 4H), 5.92 (s, 1H), 4.76–4.95 (AA′BB′, 4H; -CH_2-), 1.80 ppm (s, 3H); ^{13}C NMR (75 MHz, $CDCl_3$): δ = 154.42, 154.03, 133.70, 130.28, 130.10, 129.72, 129.66, 128.17, 128.04, 127.21, 126.59, 126.58, 126.48, 126.17, 126.14, 124.37, 122.52, 122.28, 117,75, 117.53, 65.26, 64.64, 59.07, 11.05 ppm; MS (MALDI-TOF): *m*/*z*: 460.65 [M^+]; $[\alpha]_D^{20} = -140$ (*c* = 0.05 in CH_2Cl_2); elemental analysis calcd (%) for $C_{26}H_{20}O_2S_3$: C 67.79, H 4.38.; found: C 66.96, H 4.51.

Preparation of (*S*)-5: $NaBH_4$ (0.2 g, 5.28 mmol) was cautiously added to a solution of the dithiolium salt (*S*)-**4** (2.85 g, 4.68 mmol) in anhydrous CH_3CN (40 mL) and *i*PrOH (3 mL) under nitrogen at 0 °C. The mixture was allowed to reach room temperature and stirred for 4 h. Purification by column chromatography (silica gel, petroleum ether/EtOAc 10:2) afforded (*S*)-**5** as beige crystals after drying. Yield: 2 g (93 %). M.p. 130 °C; ^{1}H NMR (300 MHz, $CDCl_3$): δ = 7.90 (d, *J* = 9 Hz, 1H), 7.85 (d, *J* = 9 Hz, 1H), 7.78 (d, *J* = 9 Hz, 2H), 7.42 (d, *J* = 9 Hz, 1H), 7.29–7.23 (m, 3H), 7.15–7.02 (m, 4H), 5.80 (s, 1H), 4.83–4.65 (AA′BB′, 4H; -CH_2-), 1.70 ppm (s, 3H); ^{13}C NMR (75 MHz, $CDCl_3$): δ = 154.40, 154.00, 133.68, 130.26, 130.07, 129.71, 129.65, 128.15, 128.02, 127.18, 126.58, 126.56, 126.45, 126.16, 126.13, 124.35, 122.48, 122.25, 117.73, 117.50, 65.25, 64.62, 59.05, 11.02 ppm; $[\alpha]_D^{20} = +136$ (*c* = 0.05 in CH_2Cl_2); MS (MALDI-TOF): *m*/*z*: 459 [M^+]; elemental analysis calcd (%) for $C_{26}H_{20}O_2S_3$: C 67.79, H 4.38; found: C 67.86, H 4.54.

Preparation of (*R,S*)-6: A solution of HBF_4 in Et_2O (54 wt %, 0.29 mL, 1.15 mmol) was added at 0 °C to a solution of (*R,S*)-**5** (0.5 g, 1.085 mmol) in acetic anhydride (5 mL) under nitrogen. The resulting dark solution was stirred for 1 h. Anhydrous Et_2O (25 mL) was then added, and the solution was left in the fridge overnight. The resulting precipitate was filtered and washed with Et_2O to yield (*R,S*)-**6**. Yield: 0.5 g (92 %). M.p. 185 °C; ^{1}H NMR (300 MHz, CD_3CN): δ = 10.93 (s, 1H), 8.05 (d, *J* = 9 Hz, 2H), 7.94 (d, *J* = 8.4 Hz, 2H), 7.69 (d, *J* = 8.7 Hz, 2H), 7.42–7.37 (m, 2H), 7.25–7.19 (m, 2H), 7.03 (d, *J* = 8.4 Hz, 2H), 5.80–5.68 ppm (AA′, *J* = 13.8 Hz, 4H; -CH_2-); ^{13}C NMR (75 MHz, CD_3CN): δ = 117.19, 156.66, 153.10, 132.95, 130.08, 129.99, 128.05, 126.65, 125.12, 124.52, 121.13, 117.05, 116.68, 62.93 ppm; elemental analysis calcd (%) for $C_{25}H_{18}BF_4O_2S_2$: C 59.89, H 3.62; found: C 58.54, H 3.42. The product is unstable and must be stored at low temperature.

Preparation of (*R*)-6: As described above for (*R,S*)-**6**. Yield: 0.52 g (96 %). M.p. 155 °C; ^{1}H NMR (300 MHz, CD_3CN): δ = 10.93 (s, 1H), 8.03 (d, *J* = 8.1 Hz, 2H), 7.93 (d, *J* = 9 Hz, 2H), 7.67 (d, *J* = 9 Hz, 2H), 7.41–7.36 (m, 2H), 7.23–7.17 (m, 2H), 7.02 (d, *J* = 8.4 Hz, 2H), 5.7–5.81 ppm (AA′, *J* = 13.8 Hz, 4H); ^{1}H NMR (300 MHz, acetone): δ = 11.52 (s, 1H), 8.07 (d, *J* = 9 Hz, 2H), 7.95 (d, *J* = 8.1 Hz, 2H), 7.87 (d, *J* = 9 Hz, 2H), 7.40 (t, *J* = 7.5 Hz, 2H), 7.25 (t, *J* = 7.5 Hz, 2H), 7.07 (d, *J* = 8.4 Hz, 2H), 6.08–5.96 ppm (AA′, *J* = 13.8 Hz, 4H; -CH_2-); ^{13}C NMR (300 MHz, CD_3CN): δ = 177.15, 156.67, 153.11, 132.95, 130.08, 129.99, 128.05, 126.65, 125.10, 124.51, 121.13, 117.05, 116.68, 62.94 ppm; $[\alpha]_D^{20} = -186$ (*c* = 0.05 in CH_2Cl_2); elemental analysis calcd (%) for $C_{25}H_{18}BF_4O_2S_2$: C 59.89, H 3.62; found: C 57.08, H 3.53. The product is unstable and must be stored at low temperature.

Preparation of (*S*)-6: A solution of HBF_4 in Et_2O (54 wt %, 1.07 mL, 3.2 mmol) was added at 0 °C to a solution of (*R,S*)-**5** (1.85 g, 4.01 mmol) in acetic anhydride (10 mL) under nitrogen. The resulting dark solution was stirred for 1 h. Anhydrous Et_2O (100 mL) was then added, and the solution was left in the fridge overnight. The resulting precipitate was filtered and washed with Et_2O to yield (*S*)-**6**. Yield: 1.9 g (95 %). M.p. 157 °C; ^{1}H NMR (300 MHz, acetone): δ = 11.44 (s, 1H), 8.05 (d, *J* = 9 Hz, 2H), 7.92 (d, *J* = 8.1 Hz, 2H), 7.86 (d, *J* = 9 Hz, 2H), 7.38 (t, *J* = 7.5 Hz, 2H), 7.21 (t, *J* = 7.5 Hz, 2H), 7.06 (d, *J* = 8.4 Hz, 2H), 6.05–5.92 ppm (AA′, *J* = 13.8 Hz, 4H); ^{13}C NMR (300 MHz, acetone): δ = 206.57, 178.66, 158.07, 154.65, 134.33, 131.28, 131.21, 129.31, 127.67, 126.55, 125.55, 122.53, 118.02, 64.13 ppm. The product is unstable and must be stored at low temperature.

Preparation of (*RR,SS,meso*)-1: Et_3N (0.193 mL, 1.396 mmol) was added at room temperature to a solution of the dithiolium salt (*R,S*)-**6** (0.35 g, 0.698 mmol) in anhydrous CH_3CN (10 mL) under nitrogen. The resulting solution and orange precipitate were stirred for 1.5 h. After the addition of water (15 mL) and stirring for an additional 1 h, the precipitate was filtered off and washed with water. After column chromatography (silica gel, CH_2Cl_2/petroleum ether 2:1), and solvent evaporation, the residue was solubilised in toluene (5 mL), petroleum ether was added and the resulting solution was left at 4 °C overnight. The orange precipitate was filtered to give **1** as diastereomeric mixture. Yield: 0.15 g (55 %). M.p. 220 °C; ^{1}H NMR (300 MHz, acetone): δ = 8.02 (d, *J* = 9 Hz, 2H), 7.93 (d,

$J=8.1$ Hz, 2H), 7.59 (d, $J=9$ Hz, 2H), 7.40–7.35 (m, 2H), 7.27–7.21 (m, 2H), 7.08 (d, $J=8.4$ Hz, 2H), 4.91–5.01 ppm (AA′, $J=13.5$ Hz, 4H; -CH_2-); ^{13}C NMR (75 MHz, acetone): $\delta=155.35$, 134.49, 131.56, 131.15, 130.52, 129.16, 127.21, 126.58, 125.08, 123.03, 118.87, 108.07, 65.18 ppm; MS (MALDI-TOF): m/z: 824.45 [M^+]; elemental analysis calcd (%) for $C_{50}H_{32}O_4S_4$: C 72.79, H 3.91; found: C 72.71, H 4.46.

When performed on a larger scale (3.5×), the crude precipitate obtained from the coupling reaction was extracted with CH_2Cl_2 (150 mL), the solution was washed with water and dried on $MgSO_4$. Concentration to 10–15 mL induced the precipitation of a first fraction (0.25 g, 22%), whereas the mother liquors, after filtration on column chromatography (silica gel, CH_2Cl_2/petroleum ether 2:1), afforded a second fraction (0.31 g, 33%). Total yield: 0.56 g (55%). Chiral HPLC analyses showed that the first fraction was composed entirely of the pure *meso*-**1**, whereas the second fraction is strongly enriched in a racemic mixture in the following ratio: (*S*)-**1**: 42%, (*R*)-**1**: 43%, *meso*-**1**: 15% (see the Supporting Information).

Preparation of (*R*,*R*)-1: As described above for (*R*,*S*)-**1**, starting from (*R*)-**6**. Yield: 0.165 g (60%). M.p. 210°C; ^{1}H NMR (300 MHz, acetone): $\delta=7.86$ (d, $J=8.7$ Hz, 2H), 7.78 (d, $J=8.1$ Hz, 2H), 7.41 (d, $J=9$ Hz, 2H), 7.25–7.20 (m, 2H), 7.11–7.06 (m, 2H), 6.94 (d, $J=8.1$ Hz, 2H), 4.75 ppm (s, 4H); ^{13}C NMR (75 MHz, acetone): $\delta=155.33$, 134.47, 131.54, 131.13, 130.50, 129.14, 127.19, 126.56, 125.06, 123.01, 118.85, 108.05, 65.16 ppm; MS (MALDI-TOF): m/z: 824.29 [M^+]; $[\alpha]_D^{20}=+316$ ($c=0.05$ in CH_2Cl_2); elemental analysis calcd (%) for $C_{50}H_{32}O_4S_4$: C 72.79, H 3.91; found: C 72.06, H 3.61.

Preparation of (*S*,*S*)-1: Et_3N (0.66 mL, 1.396 mmol) was added at room temperature to a solution of the dithiolium salt (*S*)-**6** (1.2 g, 2.39 mmol) in anhydrous CH_3CN (30 mL) under nitrogen. The resulting solution and orange precipitate were stirred for 1.5 h. After the addition of water (100 mL) and stirring for an additional 1 h, the precipitate was filtered off and washed with water. After column chromatography (silica gel, CH_2Cl_2/petroleum ether 2:1) and solvent evaporation, the residue was solubilised in toluene (5 mL), petroleum ether was added, the resulting solution was left at 4°C overnight. The orange precipitate was filtered to give (*S*)-**1**. Yield: 0.59 g (60%). M.p. 212°C; ^{1}H NMR (300 MHz, acetone): $\delta=7.87$ (d, $J=8.7$ Hz, 2H), 7.78 (d, $J=8.1$ Hz, 2H), 7.42 (d, $J=9$ Hz, 2H), 7.26–7.20 (m, 2H), 7.11–706 (m, 2H), 6.94 (d, $J=8.7$ Hz, 2H), 4.76 ppm (s, 4H); ^{13}C NMR (75 MHz, acetone): $\delta=155.34$, 134.48, 131.55, 131.14, 130.52, 129.16, 127.21, 126.57, 125.07, 123.00, 118.85, 108.05, 65.15 ppm; $[\alpha]_D^{20}=-334$ ($c=0.05$ in CH_2Cl_2); (MALDI-TOF): m/z: 824.5 [M^+]; elemental analysis calcd (%) for $C_{50}H_{32}O_4S_4$: C 72.79, H 3.91; found: C 72.15, H 3.81.

Chiral HPLC separations: Analytical chiral HPLC experiments were performed using a Lachrom Elite unit composed of an L-2130 pump, L-2200 autosampler, L-2350 oven, L-2455 DAD-detector and a Jasco OR-1590 polarimeter. Hexane and ethanol were of HPLC grade and were degassed and filtered on a 0.45 μm membrane before use. Chiralpak IA (250×4.6 mm), amylose tris(3,5-dimethylphenylcarbamate) chiral stationary phase, from Chiral Technology Europa (Illkirch, France) was used for the analyses. The sign given by the online polarimeter is the sign of the compound in the solvent used for the chromatographic separation. Retention times (t_R) in minutes, retention factors $k_i=(t_{R(i)}-t_{R(0)})/t_{R(0)}$ and enantioselectivity $\alpha=k_2/k_1$ are given. $t_{R(0)}$ was determined by the injection of tri-*tert*-butyl benzene.

The diastereomeric mixture was injected on Chiralpak IA with a mixture hexane/ethanol/chloroform (48:48:4) as eluent: flow rate = 1 mL min^{-1}, $T=25$°C. The chromatograms (see the Supporting Information) were the UV trace at 230 nm and the polarimetric trace. $t_R(-)=17.98$, $t_R(+)=19.59$, $t_R(meso)=24.67$; $k(-)=4.99$, $k(+)=5.53$, $k(meso)=7.22$.

Crystallography: Data were collected using an APEX II Bruker AXS diffractometer with $Mo_{K\alpha}$ radiation ($\lambda=0.71073$ Å). Structures were solved by direct methods (SHELXS 97)[22] and refined (SHELXL 97)[20] by full-matrix least-squares methods as implemented in the WinGX software package.[23] An empirical absorption (multi-scan) correction was applied. Hydrogen atoms were introduced at calculated positions (riding model) included in structure factor calculations but not refined. CCDC-762695 (*meso*-**1**) contains the supplementary crystallographic data for this paper. These data can be obtained free of charge from The Cambridge Crystallographic Data Centre via www.ccdc.cam.ac.uk/data_request/cif.

Electrochemistry: Cyclic voltammetry was carried out in a three-electrode cell equipped with a platinum millielectrode and a platinum wire counter-electrode. A silver wire served as a quasi-reference electrode and its potential was checked against the ferrocene/ferrocenium couple (Fc/Fc^+) before and after each experiment. The concentration of the examined compounds was 0.5 mM and the electrolytic media consisted of CH_2Cl_2 and contained 0.1 M n-Bu_4NPF_6. All experiments were performed at RT in a glove box that contained anhydrous, oxygen-free (1 ppm) argon. Electrochemical experiments were carried out by using an EGG PAR 273A potentiostat with positive-feedback compensation.

Computational details: Full-geometry optimisation with density functional theory (DFT)[24,25] calculations were performed using the hybrid Becke three-parameter exchange functional[26] and the Lee–Yang–Parr non-local correlation functional[27] (B3LYP) implemented in the Gaussian 03 (Revision D.02) program suite[28] using the 6-31G* basis set[29] and the default convergence criterion implemented in the program. The figures were generated with MOLEKEL 4.3.[30]

Acknowledgements

We thank N. Audebrand (Rennes, France) for the powder diffraction experiments and the CINES (Montpellier, France) for allocation of computing time. This work was also supported in part by the ANR (France) under contracts nos. BLAN05-0144-02 and BLAN08-3-317277. We also thank a reviewer for their insightful comments to improve this work.

[1] D. Jérome, *Chem. Rev.* **2004**, *104*, 5565–5592.
[2] O. W. Howarth, G. K. Fraenkel, *J. Am. Chem. Soc.* **1966**, *88*, 4514–4515.
[3] M. Iyoda, M. Hasegawa, Y. Miyake, *Chem. Rev.* **2004**, *104*, 5085–5113.
[4] J. O. Jeppesen, M. Brondsted Nielsen, J. Becher, *Chem. Rev.* **2004**, *104*, 5115–5131.
[5] A. Y. Ziganshina, Y. H. Ko, W. S. Jeon, K. Kim, *Chem. Commun.* **2004**, 806–807.
[6] M. Yoshizawa, K. Kumazawa, M. Fujita, *J. Am. Chem. Soc.* **2005**, *127*, 13456–13457.
[7] N. Avarvari, J. Wallis, *J. Mater. Chem.* **2009**, *19*, 4061–4076, and references therein.
[8] C. Réthoré, N. Avarvari, E. Canadell, P. Auban-Senzier, M. Fourmigué, *J. Am. Chem. Soc.* **2005**, *127*, 5748–5749.
[9] E. Coronado, J. R. Galan-Mascaros, C. J. Gomez-Garcia, A. Murcia-Martinez, E. Canadell, *Inorg. Chem.* **2004**, *43*, 8072–8077.
[10] L. Pu, *Chem. Rev.* **1998**, *98*, 2405–2494.
[11] R. Gómez, J. L. Segura, N. Martin, *J. Org. Chem.* **2000**, *65*, 7566–7574.
[12] Y. Zhou, D. Zhang, L. Zhu, Z. Shuai, D. Zhu, *J. Org. Chem.* **2006**, *71*, 2123–2130.
[13] H. Wu, D. Zhang, D. Zhu, *Tetrahedron Lett.* **2007**, *48*, 8951–8955.
[14] P. Hudhomme, S. Le Moustarder, C. Durand, N. Gallego-Planas, N. Mercier, P. Blanchard, E. Levillain, M. Allain, A. Gorgues, A. Riou, *Chem. Eur. J.* **2001**, *7*, 5070–5083.
[15] P.-T. Chiang, N.-C. Chen, C.-C. Lai, S. H. Chiu, *Chem. Eur. J.* **2008**, *14*, 6546–6552.
[16] H. Spanggaard, J. Prehn, M. B. Nielsen, E. Levillain, M. Allain, J. Becher, *J. Am. Chem. Soc.* **2000**, *122*, 9486–9494.
[17] L. Huchet, S. Akoudad, E. Levillain, J. Roncali, A. Emge, P. Bäuerle, *J. Phys. Chem. B* **1998**, *102*, 7776–7781.

[18] J. B. Torrance, B. A. Scott, B. Welber, F. B. Kaufman, P. E. Seiden, *Phys. Rev. B* **1979**, *19*, 730–741.
[19] K. Boubekeur, C. Lenoir, P. Batail, R. Carlier, A. Tallec, M.-P. Le Paillard, D. Lorcy, A. Robert, *Angew. Chem.* **1994**, *106*, 1448–1451; *Angew. Chem. Int. Ed. Engl.* **1994**, *33*, 1379–1381.
[20] Single-point energy calculations on the individual fragments of the optimised dyad show that for the neutral or for the cation radical state the energy is only around 1.5 $kcal\,mol^{-1}$ higher than that of each respective fragment in its optimised geometry. This is indicative of the flexibility of the individual fragments and of the low energy cost for the rearrangement that leads to the clip formation.
[21] N. B. Nielsen, N. Thorup, J. Becher, *J. Chem. Soc. Perkin Trans. 1* **1998**, 1305–1308.
[22] SHELX97-Programs for Crystal Structure Analysis, Release 97-2, G. M. Sheldrick, University of Göttingen, Göttingen **1998**.
[23] L. J. Farrugia, *J. Appl. Crystallogr.* **1999**, *32*, 837–838.
[24] P. Hohenberg, W. Kohn, *Phys. Rev.* **1964**, *136*, B864-B871.
[25] R. G. Parr, W. Yang, *Density-Functional Theory of Atoms and Molecules*; Oxford University Press, Oxford, **1989**.
[26] a) A. D. Becke, *Phys. Rev.* **1988**, *38*, 3098–3100; b) A. D. Becke, *J. Chem. Phys.* **1993**, *98*, 1372–1377; c) A. D. Becke, *J. Chem. Phys.* **1993**, *98*, 5648–5652.
[27] C. Lee, W. Yang, R. G. Parr, *Phys. Rev. B* **1988**, *37*, 785–789.
[28] Gaussian 03, Revision D.02, M. J. Frisch, G. W. Trucks, H. B. Schlegel, G. E. Scuseria, M. A. Robb, J. R. Cheeseman, J. A. Montgomery, Jr., T. Vreven, K. N. Kudin, J. C. Burant, J. M. Millam, S. S. Iyengar, J. Tomasi, V. Barone, B. Mennucci, M. Cossi, G. Scalmani, N. Rega, G. A. Petersson, H. Nakatsuji, M. Hada, M. Ehara, K. Toyota, R. Fukuda, J. Hasegawa, M. Ishida, T. Nakajima, Y. Honda, O. Kitao, H. Nakai, M. Klene, X. Li, J. E. Knox, H. P. Hratchian, J. B. Cross, V. Bakken, C. Adamo, J. Jaramillo, R. Gomperts, R. E. Stratmann, O. Yazyev, A. J. Austin, R. Cammi, C. Pomelli, J. W. Ochterski, P. Y. Ayala, K. Morokuma, G. A. Voth, P. Salvador, J. J. Dannenberg, V. G. Zakrzewski, S. Dapprich, A. D. Daniels, M. C. Strain, O. Farkas, D. K. Malick, A. D. Rabuck, K. Raghavachari, J. B. Foresman, J. V. Ortiz, Q. Cui, A. G. Baboul, S. Clifford, J. Cioslowski, B. B. Stefanov, G. Liu, A. Liashenko, P. Piskorz, I. Komaromi, R. L. Martin, D. J. Fox, T. Keith, M. A. Al-Laham, C. Y. Peng, A. Nanayakkara, M. Challacombe, P. M. W. Gill, B. Johnson, W. Chen, M. W. Wong, C. Gonzalez, J. A. Pople, Gaussian, Inc., Wallingford CT, **2004**.
[29] P. C. Hariharan, J. A. Pople, *Chem. Phys. Lett.* **1972**, *16*, 217–219.
[30] MOLEKEL 4.3, P. Flükiger, H. P. Lüthi, S. Portmann, J. Weber, Swiss National Supercomputing Centre CSCS, Manno, **2000**.

Received: July 23, 2009
Revised: January 28, 2010
Published online: June 2, 2010

